EurJIC European Journal of Inorganic Chemistry

DOI: 10.1002/ejic.201200075

The Solution Chemistry of Cu^{2+}–tren Complexes Revisited: Exploring the Role of Species That Are Not Trigonal Bipyramidal

Carmen E. Castillo,[a,b] Andrés G. Algarra,[a] M. Ángeles Máñez,[a] Carole Duboc,[b] and Manuel G. Basallote*[a]

Keywords: Copper complexes / Kinetics / UV/Vis spectroscopy / Density functional calculations / EPR spectroscopy

Potentiometric and spectrophotometric titrations indicate that aqueous solutions that contain equimolar amounts of Cu^{2+} and tren contain the $HCuL^{3+}$, CuL^{2+} and $CuL(OH)^{+}$ species and that their relative concentrations depend on the pH of the solution. The stability constants and the UV/Vis and EPR spectra of the three species have been determined. The position of the absorption maximum clearly corresponds to a trigonal bipyramidal (tbp) geometry for CuL^{2+}, whereas for $HCuL^{3+}$ and $CuL(OH)^{+}$ there are also bands that could correspond to square pyramidal (sp) complexes, but the EPR spectra indicate that only $HCuL^{3+}$ can be considered to be sp. When any of these species is mixed with an excess of acid, an intermediate is formed within the mixing time of the stopped-flow technique. This intermediate undergoes complete decomposition in a second slower step. Interestingly, the spectrum of this intermediate is typical of sp geometry. Kinetic studies on complex formation in general indicate that complexation occurs in a single step, although under certain conditions an additional step has been observed that probably corresponds to the conversion of CuL^{2+} to $HCuL^{3+}$, and the spectral changes indicate that the process involves structural reorganization from tbp to sp geometry. DFT and TD-DFT calculations have been carried out for the three stable species, as well as for species in a higher protonation state. The results indicate that CuL^{2+} exists as a species with tetradentate tren and tbp geometry, although a wide range of distortions between the ideal tbp geometry and a geometry closer to sp is possible with a very modest energy cost. The energy change associated with hydrolysis of one of the Cu–N bonds to give a species with tridentate tren was found to be slightly higher than that previously found for a related ligand, which contains a substituent at one of the terminal amino groups. For $CuL(OH)^{+}$, the calculations suggest that an equilibrium exists between species with essentially the same energy but different geometries, each one of the species is closer to one of the ideal tbp and sp limits. For $HCuL^{3+}$, the relevance of the sp geometry was confirmed by the calculations.

Introduction

Cu^{2+} complexes show a variety of coordination geometries, which include octahedral, distorted tetragonal,[1] distorted trigonal prismatic,[2] square planar[3] and tetrahedral geometries.[4] Despite the relevance of these geometries, complexes with open chain and macrocyclic polydentate amine ligands frequently show a coordination number of five.[5–7] Moreover, this coordination number is not limited to polyaza ligands, and combined neutron diffraction and molecular dynamics studies by Pasquarello et al.[8] suggests that $[Cu(aq.)]^{2+}$ can be also a five-coordinate complex. Structural studies indicate that this coordination number covers a continuum between the idealized trigonal bipyramidal (tbp) and square pyramidal (sp) geometries. Tripodal tetradentate ligands, such as tris(2-aminoethyl)amine (tren) and tris(2-dipyridilmethyl)amine (tpa), favour tbp coordination.[6] However, complexes that have other polyamines show geometries that are closer to sp coordination. Because of the variety of structural distortions between the ideal tbp and sp geometries, a parameter (τ) was introduced by Addison et al. in order to quantitatively measure these distortions. The τ values are calculated with Equation (1), where α and β correspond to the two largest L–M–L bond angles in the structure,[9] so that complexes with an ideal sp structure have $\tau = 0$, those with ideal tbp coordination have $\tau = 1$ and complexes with intermediate geometries show values between 0 and 1.[2]

$$\tau = (\alpha - \beta)/60 \quad (1)$$

In the case of Cu^{2+} complexes with the tripodal ligand tren (L), the structures of many complexes with the formula $Cu(tren)X^{z+}$ (X = monodentate ligand) have been solved and they show τ values between 0.46 and 1.00. This shows that these complexes can be essentially described as being

[a] Departamento de Ciencia de los Materiales e Ingeniería Metalúrgica y Química Inorgánica, Facultad de Ciencias, Universidad de Cádiz, Polígono Universitario Río San Pedro, Puerto Real, 11510 Cádiz, Spain
E-mail: manuel.basallote@uca.es
[b] Université Joseph Fourier Grenoble 1/CNRS, Département de Chimie Moléculaire, UMR-5250, Institut de Chimie Moleculaire de Grenoble FR-CNRS-2607, Laboratoire de Chimie Inorganique Redox,
BP 53, 38041 Grenoble Cedex 9, France

Supporting information for this article is available on the WWW under http://dx.doi.org/10.1002/ejic.201200075.

tbp with more or less important distortions, but that they never approach the sp limit.[6]

Electronic spectra are usually considered to be an easy way of determining the geometry of these complexes in solution because the position of the absorption band changes with the coordination geometry and the nature of the donor atoms. Cu^{2+}–polyamine complexes with sp geometry usually have absorption bands centred at 580 to 670 nm,[7,10] whereas related tbp complexes have the band at lower energies (780–950 nm).[7,11,12] However, the major absorption band for a complex with a given geometry is sometimes accompanied by a weaker shoulder in the region that corresponds to the other geometry.[12,13] Although this feature can be interpreted by considering that the weaker band is inherent to the species whose structure is revealed in the X-ray analysis, we have recently shown for the related L1 ligand[7] (Scheme 1) that the presence of two bands in the electronic spectra can be caused by the existence of a mixture of species with different geometries in solution. In that work we observed that the Cu^{2+} complex of the tren-derived ligand that contains a quinoline substituent shows two bands centred at 890 and 660 nm in solution, which can be associated with the existence in solution of species with two different geometries. DFT calculations revealed that the effect cannot be associated with the quinoline substituent and preliminary DFT calculations for the Cu^{2+}–tren complex indicated that the same effect can be expected for complexes with unsubstituted tren. In this paper we report experimental and more detailed DFT studies that aimed to explore this possibility.

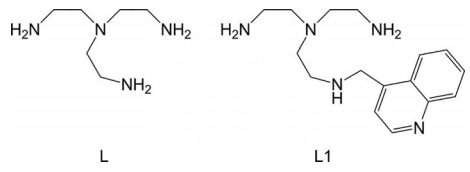

Scheme 1.

Results and Discussion

Stability, Electronic and EPR Spectra of Cu^{2+}–tren Complexes in Aqueous Solution

The equilibrium constants for both the protonation of tren and the formation of its Cu^{2+} complexes were determined from potentiometric titrations. The results are included in the Supporting Information together with the distribution curves of the corresponding species. According to these results, aqueous solutions that contain equimolar amounts of Cu^{2+} and tren contain almost exclusively the CuL^{2+} form at a pH close to 7, whereas in basic solutions it converts completely to $CuL(OH)^{+}$. In slightly acidic solutions, significant amounts of $HCuL^{3+}$ form, although it never represents more than 30% of the total ligand species. These results are in good agreement with previously reported values for the protonation constants of the ligand and the formation of the CuL^{2+} and $CuL(OH)^{+}$ species.[14] However, formation of the $HCuL^{3+}$ species has been only rarely proposed for tren itself,[14b,14c] although it has been proposed for related ligands.[15] Nevertheless, some complexes that contain monoprotonated tren have been structurally characterized.[16] The $\log K$ value derived in this work for the formation of $HCuL^{3+}$ from CuL^{2+} (3.98) is in good agreement with those values reported in the literature (3.63–4.06).[14b,14c] As it was considered fundamental for the purposes of the present study to determine the nature and electronic spectra of the different species formed in solution, a spectrophotometric titration in which the pH dependence of the spectra of solutions that contain Cu^{2+} and tren in a 1:1 molar ratio was carried out. The spectra of these solutions always show a broad absorption band that expands from ca. 600 to 900 nm, but significant changes in the position of the maximum, and especially in the relative absorptivity in the 600 to 700 nm and the 750 to 900 nm ranges, were observed when the pH was changed. Analysis of the data provided refined values for the equilibrium constants of the three complexes that are in quite good agreement with those determined from potentiometric titrations (Table S1, Supporting Information) and also provided the electronic spectra for each Cu^{2+}–tren species (Figure 1). It is important to note that the $HCuL^{3+}$ spectrum is subject to larger errors than the CuL^{2+} and $CuL(OH)^{+}$ spectra because $HCuL^{3+}$ is only formed as a minor species in solution. The resolved spectra clearly indicate that CuL^{2+} shows a maximum centred at 840 nm with a weak shoulder around 660 nm, $CuL(OH)^{+}$ shows two overlapping bands centred at ca. 850 and 680 nm, and $HCuL^{3+}$ shows a maximum at ca 660 nm with a broad absorption that extends up to 900 nm. The appearance of two components associated with the formation of the hydroxo complex has been noted previously,[17] and it was interpreted in terms of distortion from a trigonal bipyramidal structure in CuL^{2+} to a more square pyramidal structure in the hydroxo complex. To the best of our knowledge, the resolved spectrum for the protonated $HCuL^{3+}$ species has not been previously reported.

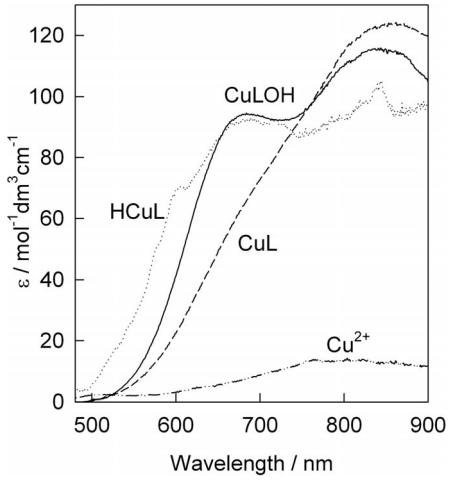

Figure 1. Absorption spectra of the $HCuL^{3+}$ (dotted line), CuL^{2+}(dashed line) and $CuLOH^{+}$ (solid line) complexes obtained from the analysis of the spectophotometric titration.

This resolved spectrum for the protonated $HCuL^{3+}$ species also suggests a structure closer to the square pyramid. The reported crystal structures of $[Cu(HL)Cl_2](ClO_4)\cdot H_2O$ and $[Cu_2(HL)_2Cl_2](nds)_2\cdot 5H_2O$[16] ($nds^{2-}$ = naphthalene-1,5-disulfonate), in which the coordination environments around Cu^{2+} are essentially square pyramidal (τ values of 0.083 for the monomer, and 0.313 and 0.331 for the two Cu of the dimer), are in agreement with this conclusion.

As these results seem to imply that the chemistry of Cu–tren complexes is not necessarily related exclusively to the tbp geometry, additional evidence of species with sp geometry needed to be obtained with an additional technique. Thus, EPR was selected because it is one of the most suitable techniques for studying the stereochemistry of paramagnetic complexes in solution. In general, EPR spectra of sp complexes are characterized by an axial pattern with the features $g_{\|} > 2.1 > g_{\perp} > 2.0$ and $A_{\|} = (120–150)\times 10^{-4}$ cm^{-1}, whereas complexes with the tbp structure typically show EPR spectra that are characterized by a "reversed axial" appearance with $g_{\|} > g_{\perp} \approx 2.0$ and $A_{\|} = (60–100)\times 10^{-4}$ cm^{-1}.[16,18] Therefore, the coordination geometry around the central Cu^{II} ion can be deduced from the analysis of its EPR spectral features.

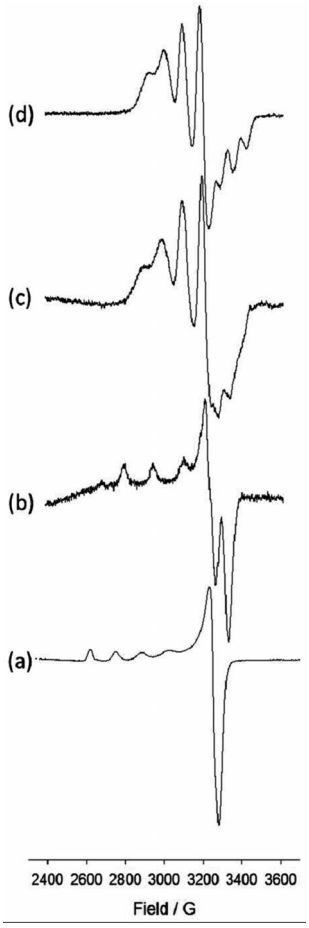

Figure 2. Frozen solution EPR spectra of the Cu–tren species: (a) Cu_{aq}^{2+}, (b) $HCuL^{3+}$, (c) CuL^{2+} and (d) $CuL(OH)^{+}$.

The EPR spectra of frozen solutions that contain Cu^{2+} and tren in a 1:1 molar ratio (10^{-3} M concentration) at different pHs were recorded and are included in the Supporting Information. From these spectra, the EPR spectra of the four Cu-containing species were calculated by using the procedure indicated in the Experimental. The resulting spectra are shown in Figure 2 and the derived parameters are collected in Table 1. It is evident that the spectral patterns observed for the Cu_{aq}^{2+} and $HCuL^{3+}$ species are different from those obtained for the CuL^{2+} and $CuL(OH)^{+}$ complexes.

Table 1. EPR parameters of the Cu-containing species that exist in solutions that contain Cu^{2+} and tren in a 1:1 molar ratio at different pH values.

Species	$g_{\|}$	$g_{\perp}$	$g_{\|}$	$A_{\|}$ [cm^{-1}]	$A_{\perp}$ [cm^{-1}]
Cu_{aq}^{2+}	2.397	2.081	2.397	0.0142	–
$HCuL^{3+}$	2.235	2.058	2.235	0.0179	–
CuL^{2+}	2.016	2.203	2.016	0.0055	0.0115
$CuL(OH)^{+}$	2.004	2.199	2.004	0.0064	0.0103

The latter species show EPR spectra that are consistent with the tbp geometry that was suggested by the UV/Vis spectra, the spectrum of $HCuL^{3+}$, however, shows that $g_{\|} > 2.1 > g_{\perp} > 2.0$ and $A_{\|} = (120–150)\times 10^{-4}$ cm^{-1}, which strongly suggests a square pyramidal geometry.

The Kinetics of the Acid-Promoted Decomposition of Cu^{2+}–tren Complexes

The speciation curves in Figure S1 (see Supporting Information) show that addition of an excess of acid to a solution of the Cu^{2+}–L complexes must result in complex decomposition according to Equation (2). The kinetics of this kind of decomposition process have been widely studied in the literature,[19,20] and we have previously shown that, in addition to information about the decomposition process, it can also provide valuable information about the molecular reorganization processes.[19]

$$CuL^{2+} + 3\ H^{+} \rightarrow Cu^{2+} + H_3L^{3+} \quad (2)$$

The species distribution curves were used to determine the pH values at which solutions of Cu^{2+} and tren in a 1:1 molar ratio contain the different Cu^{2+}–tren complexes ($HCuL^{3+}$, CuL^{2+} and $CuLOH^{+}$) as the major complex species. Solutions prepared under these conditions were then mixed in a stopped-flow instrument with an excess of acid and the spectral changes that correspond to complex decomposition were monitored. Very rapid absorbance changes occurred during the mixing time of the stopped-flow instrument (ca. 1.7 ms) and were observed during the decomposition of all three species. As a result of these changes, the spectra recorded immediately after mixing in the stopped-flow instrument were different from those that correspond to the Cu^{2+}–tren complexes in Figure 1. In all of the cases the initial spectra recorded in these kinetic ex-

periments show a band centred at 630 nm (Figure 3), which indicates the formation of a common intermediate (I) for the decomposition of all of the studied species. In a subsequent step, the band centred at 630 nm disappears with spectral changes that can be fitted satisfactorily by a single exponential to obtain k_{2obs} values that are independent of the starting pH and that show a linear dependence with respect to the acid concentration (Figure 4), [Equation (3)]. The value derived for the second-order rate constant (k_2) from analysis of the whole set of decomposition experiments is $(1.50 \pm 0.01) \times 10^3$ M^{-1} s^{-1}. In view of a recent report that showed the formation of complexes between nitrate and the protonated forms of tren,[21] there is the possibility that the NO_3^- anions introduced in the metal salt play some role in the decomposition process. For this reason, some kinetic experiments were carried out by using $CuCl_2$ as the metal source, HCl as the acid and 0.15 M Me_4NCl as the supporting electrolyte, and no differences were observed in the kinetic results (Figure S4, Supporting Information). Moreover, the kinetic results remained unaffected when Me_4NCl was replaced with KNO_3 as the supporting electrolyte, which shows that nitrate (or chloride) anions do not affect the kinetics of complex decomposition. The reasons for this behaviour are probably related to the fact that anion complexation by the ligand only occurs once tren is released from the complex and becomes protonated. On the other hand, anion coordination to the metal (structurally confirmed in the case of Cl^-),[16] appears to have a negligible effect on complex decomposition, probably because the anions used are not very sterically demanding and so they do not introduce significant additional strain to the Cu–N bonds.

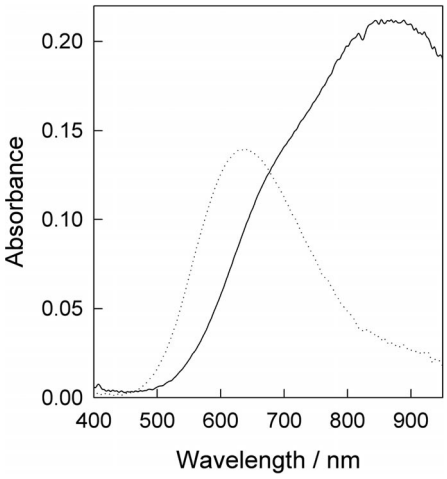

Figure 3. Absorption spectra of the CuL^{2+} complex (continuous line) and the intermediate formed immediately after mixing it with an acid excess in the stopped-flow instrument (dotted line).

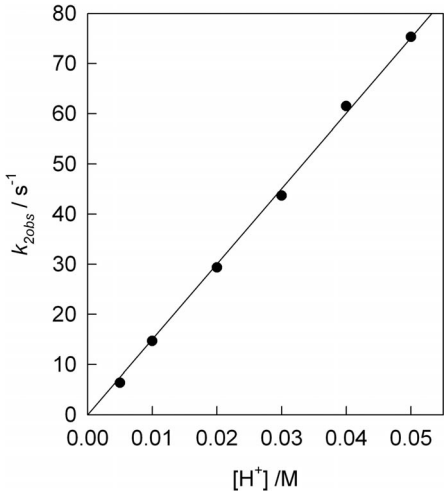

Figure 4. Plot of the dependence of the observed rate constant on the acid concentration in the second kinetic step during the acid-promoted decomposition of the $HCuL^{3+}$, CuL^{2+} and $CuLOH^+$ complexes, ([$NaClO_4$] = 0.15 M, 25.0 °C).

$$k_{2obs} = k_2 \times [H^+] \quad (3)$$

The experimental rate law observed for the decomposition of the intermediate is a simplification of the widely observed one [Equation (4)], and can be rationalized according to the mechanism in Equations (5), (6) and (7).[22] In general, following the initial formation of an activated intermediate in which the Cu–N bond is not completely broken [Equation (5)], complex decomposition is achieved through two parallel pathways involving acid [Equation (6)] and water [Equation (7)] attacks. If the $(M–L)_{INT*}$ activated intermediate is assumed to be formed under steady state conditions, then the rate law in Equation (4) is derived. Nevertheless, the absence of a nonzero intercept in the plot of Figure 4 indicates that the intermediate, which is generated during decomposition of the Cu^{2+}–tren complexes, decomposes exclusively through the proton-assisted pathway. As the only rate constant that can be resolved from the experimental data (k_2) corresponds to the product $K_{d1} \times k_H$, no more details about the intimate mechanism of decomposition could be obtained.

$$k_{obs} = \frac{k_{d1} k_{H_2O} + k_{d1} k_H [H^+]}{k_{-d1} + k_{H_2O} + k_H [H^+]} \quad (4)$$

$$(M–L)_{INT} \leftrightarrows (M–L)_{INT*}\ k_{d1}, k_{-d1}: K_{d1} \quad (5)$$

$$H^+ + (M–L)_{INT*} \rightarrow M + LH\ k_H \quad (6)$$

$$H_2O + (M–L)_{INT*} \rightarrow M + L\ k_{H_2O} \quad (7)$$

Independent of the intimate mechanism for complex decomposition, the data in this work indicate that decomposition of the different Cu^{2+}–tren complexes occurs with biphasic kinetics, although the first step is too fast for the rate constant to be measured with the stopped-flow technique. It is interesting to note that a previous report on the kinetics of the decomposition of the Cu^{2+}–tren complexes indicated the existence of a step with rate constants close to those found in this work. However, these experiments were carried out at a single wavelength and no indication

was made about the occurrence of faster absorbance changes within the mixing time of the instrument, thus the formation of the transient intermediate with an absorption maximum at 630 nm was unnoticed.[23] On the other hand, the kinetic behaviour of the tren complexes resembles that of the related L1 complexes,[7] whose decomposition shows a faster disappearance of the absorption band at 890 nm compared to the overlapping absorption at 660 nm. The kinetic analysis revealed two forms of $CuL1^{2+}$ in solution, one with tbp geometry (890 nm) and the other with sp geometry (660 nm). When acid was added, there was complete conversion to the species with sp geometry, which decomposed in a second step. In that case, the DFT study revealed that the initial rapid step is related to an equilibrium of the hydrolysis of the Cu–N bond with the amino group that supports the quinoline ring, thus $CuL1^{2+}$ is actually a mixture of $[CuL1(H_2O)]^{2+}$ and $[CuL1(H_2O)_2]^{2+}$.

In an attempt to obtain some information about the kinetics of the rapid step for the tren complex, some stopped-flow experiments were carried out by mixing solutions that contained the Cu^{2+}–tren complexes with chloroacetate/chloroacetic acid buffered solutions, which covered a pH range of 2.6 to 3.2. The spectral changes observed in these experiments showed the initial disappearance of the band typical of Cu^{2+}–tren complexes (centred at 850 nm) with the formation of intermediate I (band at 630 nm). Following this initial step, there are further complex spectral changes that probably correspond to coordination of chloroacetate. These changes were not analyzed in detail. Unfortunately, the spectral changes observed during the formation of I were still quite fast (a few milliseconds) even at the low $[H^+]$ used in these experiments, which once again hindered a kinetic study of this step.

The most important observation from the point of view of this work is the formation of an intermediate during the decomposition of the Cu^{2+}–tren complexes that shows an absorption band centred at 630 nm, a wavelength far from those typical of tbp Cu^{2+} complexes. In accordance with the conditions in which it is formed, this intermediate must be a protonated species of the form $H_xCuL^{(2+x)+}$, although the value of x cannot be deduced from the information available. The absorption maximum is close to that observed for $Cu(dien)^{2+}$ (625 nm),[23,24] which suggests a tridentate coordination of tren in intermediate I. However, as the same intermediate is also formed in the decomposition of the $HCuL^{3+}$ species, which already contains tridentate tren, it can be supposed that I corresponds to a metastable H_2CuL^{4+} species with tren acting as bidentate, which is not detectable with the potentiometric studies. In fact, the values of k_{2obs} in Figure 4 are close to those observed for the decomposition of $Cu(en)^{2+}$,[23] which also shows an absorption band at 630 to 650 nm.[25] An alternative possibility is that I is an unstable isomeric form of the $HCuL^{3+}$ species detected in the potentiometric equilibrium studies.

The Kinetics of Formation of Cu^{2+}–tren Complexes

The kinetics of complex formation was studied over the pH range of 4.0 to 5.5 and also in strongly basic solutions. In order to make complex formation slow enough to be measured with the stopped-flow instrument, the kinetic studies were conducted under non-pseudo first-order conditions, that is, by using stoichiometric concentrations of the metal ion and the ligand. No buffer was employed because it has been observed that the addition of buffer in this kind of measurement often introduces some complications.[26,27] The formation of the complex was followed by the appearance of its characteristic band in the UV/Vis spectrum.

For the experiments under acidic conditions, independent of the starting pH, the process occurred with spectral changes (Figure 5) that could be satisfactorily fitted by the simple kinetic model in Equation (8) with a second-order rate constant that is independent of pH and has a k_1 value of $(2.3 \pm 0.1) \times 10^3$ M^{-1} s^{-1}. As tren exists exclusively as H_3L^{3+} under these experimental conditions, it was concluded that k_1 corresponds to complex formation between this species and Cu^{2+}.[28] The value of k_1 is in reasonable agreement with that reported many years ago by Roche and Wilkins, who estimated a rate constant in the order of 10^2 M^{-1} s^{-1} for complex formation from Cu^{2+} and triprotonated tren.[14a] The difference in these two rate constants is easily understood given the different experimental conditions used (acetate-buffered solutions that cover a pH range where the major contribution to complex formation comes from H_2tren^{2+}).[14a] Moreover, Kaden and coworkers[29] re-evaluated the kinetic data of Roche and Wilkins and reported an estimation of 1.44×10^3 M^{-1} s^{-1} for the rate constant for the reaction between Cu^{2+} and H_3tren^{3+}, which is closer to the value obtained in this work. In any case, the value is significantly smaller than those reported for the interaction of Cu^{2+} with other tripositive ligand species.[30]

$$H_3L^{3+} + Cu^{2+} \rightarrow CuL^{2+} + 3\ H^+ \quad k_1 \qquad (8)$$

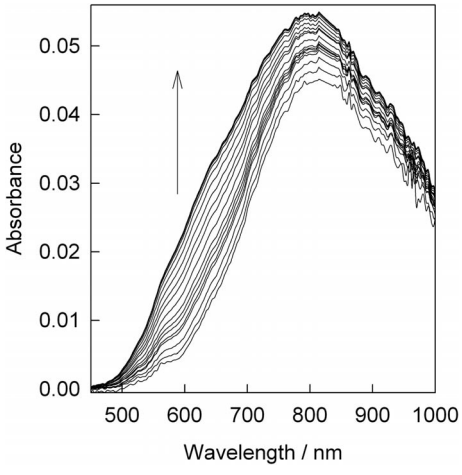

Figure 5. Typical spectral changes observed during the formation of the Cu^{2+}–tren complexes in acidic solutions ($[Cu]_0 = [L]_0 = 1.0 \times 10^{-3}$ M, 25.0 °C, 0.10 M $NaClO_4$, starting pH = 5.5). The spectra were acquired by using a logarithmic time base of 10 s, although for simplicity only some of them are plotted.

In order to check the possibility of a significant effect of nitrate anions on the kinetics of complex formation, some experiments were carried out by mixing solutions that con-

tained equimolar amounts of $CuCl_2$ and tren at pH between 4.0 and 5.5, both in the absence and the presence of added nitrate (up to an excess of 0.05 M). The results of these experiments did not show any significant effect of the added nitrate. The value of the whole set of experiments was $(1.9 \pm 0.4) \times 10^3$ $M^{-1} s^{-1}$. Although the interaction of nitrate with the protonated forms of tren is expected not to affect the kinetics of complex decomposition, the same is not necessarily true for complex formation because anion coordination is expected to change the capability of the H_3L^{3+} species to form the outer sphere complex, both for electrostatic and steric reasons. The absence of a significant effect in this kinetic study is thus somewhat surprising, although it can be understood if it is considered that H_3L^{3+} is also able to interact with other anions that would yield adducts in which the anion interacts with the protonated amino groups and that places the lone pair on the tertiary nitrogen inside the ligand cavity.[21] This would severely hinder its ability to interact with the metal centre.

With regards to the complex species formed in the kinetic studies in the acidic solutions, the species diagrams in Figure 1 anticipate the formation of a mixture of $HCuL^{3+}$ and CuL^{2+}, although the relative amount of $HCuL^{3+}$ is expected to be larger than that corresponding to the starting pH because the absence of buffer allows for acidification during complex formation. In agreement with these expectations, the final spectra in these kinetic experiments show a maximum at 780 to 800 nm (Figure 5) that coincides reasonably well with that expected for the formation of a mixture of $HCuL^{3+}$ and CuL^{2+} species. Unfortunately, these experiments did not provide any evidence for the existence of kinetically resoluble steps that correspond to reorganization between complexes with different geometries. Similar spectral changes were observed for copper complex formation with L1.[7] The reaction between Cu^{2+} and the ligand (L1) in acidic media led to the evolution of a broad band centred at 800 nm, which is typical of tbp coordination. Analysis of the kinetic data revealed the contribution of H_3L1^{3+} and H_4L1^{4+} to complex formation with rate constants of 1.26×10^3 and $5.3 \pm 0.6 \times 10^2$ $M^{-1} s^{-1}$, respectively, which is in agreement with the value found in this work for triprotonated H_3L^{3+}, $(2.3 \pm 0.1) \times 10^3$ $M^{-1} s^{-1}$.

In an attempt to obtain additional information about possible structural reorganizations during complex formation, some kinetic experiments were carried out by mixing Cu^{2+} solutions at a pH of 5.0 with ligand solutions at higher pH values (5–8). As there is formation of significant amounts of Cu^{2+} hydroxo complexes under these conditions,[31] an increase in the rate of complex formation must be expected from electrostatic considerations. In fact, the appearance of the band at ca. 850 nm for CuL^{2+} occurs within the mixing time of the stopped-flow instrument, but the reaction continues with slower spectral changes that can be attributed to the conversion of CuL^{2+} to $HCuL^{3+}$, which is caused by the pH decrease associated with complexation in the absence of a buffer (Figure 6). The process occurs with a rate constant of 4.8 ± 0.6 s^{-1}, which does not show significant changes between experiments at different starting pH values, and it clearly indicates the existence of a kinetically resolvable step that is associated with structural reorganization between complexes with tbp and sp geometries. It was surprising that the conversion to $HCuL^{3+}$ is more evident in these experiments than in those carried out at lower pH values, where the relative amount of this species must be higher. However, at lower pH values the rate of complexation becomes slower than the reaction between CuL^{2+} and H^+ to form $HCuL^{3+}$, and thus the spectral changes only reveal the formation of an equilibrium mixture of both complexes.

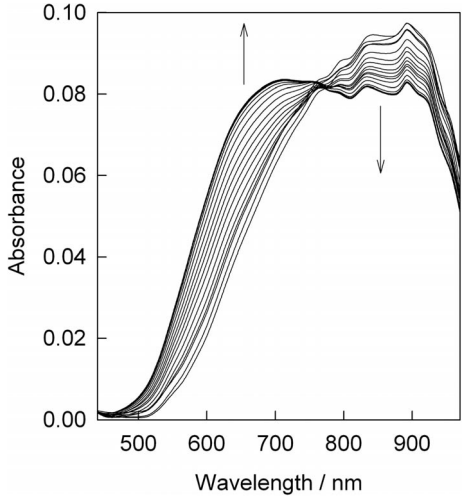

Figure 6. Typical spectral changes observed in the kinetic experiments of the formation of Cu^{2+}–tren complexes at intermediate pH values ($[Cu]_0 = [L]_0 = 1.0 \times 10^{-3}$ M, 25.0 °C, 0.10 M $NaClO_4$, starting pH = 7). The spectra were acquired by using a logarithmic time base of 10 s, although for simplicity only some of them are plotted. These changes follow an initial step that occurs within the mixing time of the instrument, which leads to the appearance of the band at ca. 850 nm.

In order to complete the kinetic studies on complex formation, some experiments were carried out in strongly basic solutions, where the ligand exists in the completely deprotonated form (L) and Cu^{2+} exists as a mixture of $Cu(OH)_3^-$ and $Cu(OH)_4^{2-}$.[32,33] Under these conditions the spectral changes (Figure 7) revealed the existence of a single second-order step (first-order with respect to each of the reactants) with a constant k_{obs} of 46 ± 6 $M^{-1} s^{-1}$ at a pH of 12.5.

Attempts to carry out the experiments at lower pH values were unsuccessful because of solubility problems and so the contributions of the tri- and tetrahydroxo Cu^{2+} species could not be separated. The value of k_{obs} is significantly smaller than those measured for other polyamines, namely 1.0×10^7 $M^{-1} s^{-1}$ for 1,4,8,11-tetrazaundecane, 2.7×10^6 $M^{-1} s^{-1}$ for 1,4,8,11-tetrazacyclotetradecane (cyclam), 2.2×10^6 $M^{-1} s^{-1}$ for a binucleating macrocycle that contained two dien subunits, 4.0×10^5 $M^{-1} s^{-1}$ for 1,1,7,7-tetraethyldiethylenetriamine and 3.1×10^3 $M^{-1} s^{-1}$ for (N-Me_4)cyclam [all of the values correspond to the contribution of $Cu(OH)_3^-$, the $Cu(OH)_4^{2-}$ values are typically one to two orders of magnitude smaller].[33,34] It is especially

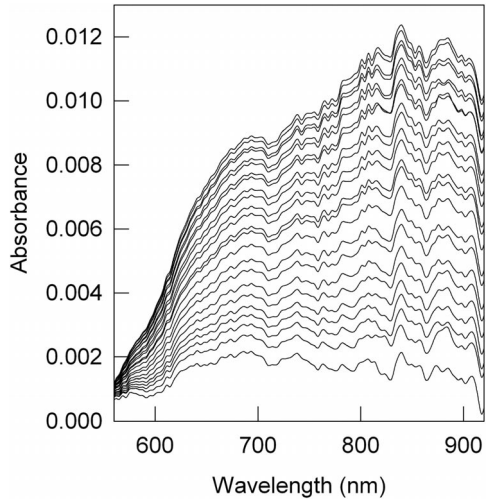

Figure 7. Spectral changes observed in the kinetic experiments of the formation of Cu^{2+}–tren complexes in strongly basic solutions ($[Cu]_0 = [L]_0 = 1.0 \times 10^{-4}$ M, 25.0 °C, 0.10 M $NaClO_4$, starting pH = 12.5). The spectra were acquired by using a logarithmic time base of 500 s, although for simplicity only some of them are plotted.

interesting to note that complexation with tren is several orders of magnitude slower than with 1,4,8,11-tetrazaundecane despite the fact that both ligands have unprotonated primary amine donors that are able to interact with the metal centre, which confirms previous proposals in the sense that the mechanisms of reaction under these conditions are complex and can differ appreciably in the position of the rate-determining step.[35] From the point of view of this work, it must be noted that the final spectrum in these kinetic experiments coincides with that of $CuL(OH)^+$ in Figure 1, and the spectral changes show the gradual increase of the major absorption band and the shoulder, that is, they do not show evidence of formation of any intermediate.

DFT Study

The kinetic results in the previous sections are rather similar to those previously obtained for the related L1 ligand, which has a quinoline substituent at one of the terminal amino groups of tren.[7] The DFT studies for the related L1 ligand indicate that the quinoline ring plays a passive role because it is unable to coordinate to the metal centre for steric reasons. In order to complement the experimental study, the most stable geometries for $HCuL^{3+}$, CuL^{2+} and $CuLOH^+$ have been optimized in solution by using DFT procedures, which started with both tetra- and tridentate ligand coordination modes and included the water ligands required to complete a coordination number of five.[36] A recent theoretical study at the DFT(B3LYP) level of theory on the first protonation step of a series of Cu^{II} complexes with various tripodal tetraamines showed that $CuL(H_2O)^{2+}$ and $Cu(HL)(H_2O)_2^{3+}$, both of which have a coordination number of five, are the most stable species

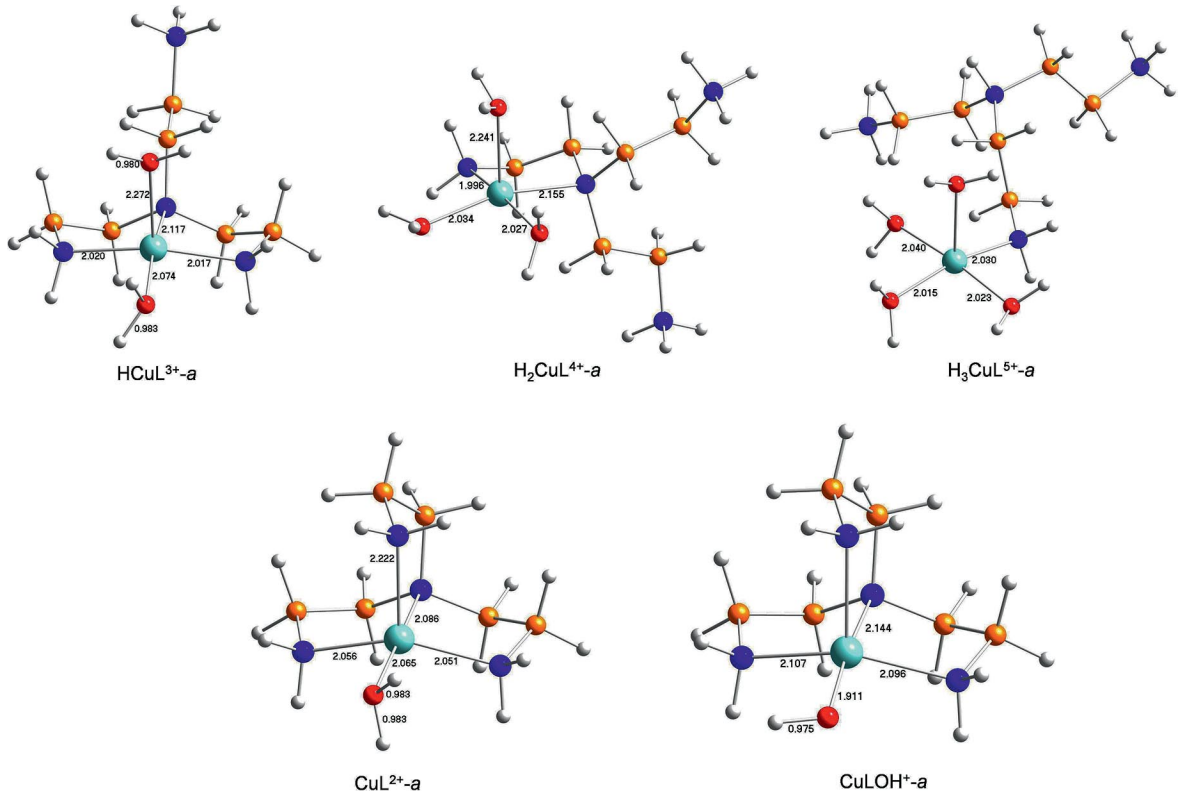

Figure 8. Solution optimized geometries for the CuL^{2+}, $HCuL^{3+}$, H_2CuL^{4+}, H_3CuL^{5+} and $CuLOH^+$ species described in the text. Only the most stable of the geometries found for each species is shown, the remaining geometries are included in the Supporting Information. The colour code is copper (cyan), nitrogen (blue), carbon (orange), oxygen (red) and hydrogen (white).

and that there is a correlation between the solvent–proton affinity of $[Cu(L)(H_2O)]^{2+}$ complexes and the formation constants for $[Cu(HL)(H_2O)_2]^{3+}$ complexes. Therefore, along with the protonation of $[Cu(L)(H_2O)]^{2+}$ complexes in solution, a molecule of water is added to the complex.[37] During the acid-promoted decomposition of the complexes there is formation of an intermediate that could correspond to a higher protonated species, thus, H_2CuL^{4+} and H_3CuL^{5+} were also included in the calculations. The structure of the most stable geometry that was optimized for each species is presented in Figure 8, whereas Table 2 includes the τ values and the relative energy in solution for all of the optimized geometries that were found for each of the species. In an effort to simulate the water media, optimizations were carried out by including solvent effects by the CPCM method.[38] Nevertheless, solvent specific interactions have not been included and therefore the energy values must be considered with caution. The wavelength of the most intense transition for each geometry was calculated by employing TD-DFT methodology and the values are also included in Table 2 (see Computational Details). In general, the calculated spectra only show a transition within the wavelength range where the typical bands for these compounds appear. However, in some cases two separate bands are expected and they are indicated in Table 2. Detailed listings of the Cartesian coordinates, excitation energies and oscillator strengths are given in the Supporting Information.

Table 2. Summary of relative energies (E_{rel}), τ, λ_{max} [nm] and oscillator strengths (f) for the different solution optimized geometries that were obtained for the pentacoordinate CuL^{2+}, $HCuL^{3+}$, H_2CuL^{4+}, H_3CuL^{5+} and $CuLOH^{+}$ species described in the text.

Species	E_{rel}	τ	λ_{max} [nm][a]	10^3 f
$CuLOH^{+}$-*a*	0.0	0.35	608.49	3.1
$CuLOH^{+}$-*b*	1.0	0.82	807.79[b]	2.2
$CuLOH^{+}$-*c*	3.6	0.21	688.55	3.4
CuL^{2+}-*a*	0.0	0.43	683.05	3.6
CuL^{2+}-*b*	0.6	0.58	758.72	4.0
CuL^{2+}-*c*	1.0	0.80	884.29	3.6
CuL^{2+}-*d*	5.4	0.14	557.28	2.6
CuL^{2+}-*e*	7.9	0.11	449.95[c]	19.8
CuL^{2+}-*f*	9.7	0.29	461.34[d]	21.6
CuL^{2+}-*g*	10.2	0.49	680.50	2.3
$HCuL^{3+}$-*a*	0.0	0.11	580.98	2.0
$HCuL^{3+}$-*b*	3.0	0.20	[e]	
$HCuL^{3+}$-*c*	4.9	0.36	641.67	2.8
$HCuL^{3+}$-*d*	7.3	0.27	663.73	4.0
$HCuL^{3+}$-*e*	8.8	0.51	737.36	4.0
H_2CuL^{4+}-*a*	0.0	0.10	632.68[f]	1.0
H_2CuL^{4+}-*b*	2.2	0.32	714.60[g]	1.3
H_3CuL^{5+}-*a*	0.0	0.15	646.31	0.4
H_3CuL^{5+}-*b*	3.3	0.24	697.77	0.6
H_3CuL^{5+}-*c*	5.9	0.89	852.04	1.1

[a] These values correspond to the λ [nm] of the most intense transition of each calculated spectra with the CPCM/TD-DFT approach. All of the calculated excited state energies and oscillator strengths are included in the Supporting Information. [b] The calculated spectrum shows two transitions of lower intensity at 590.21 nm (f = 0.0015) and 647.80 nm (f = 0.0011). [c] The calculated spectrum shows a transition of lower intensity at 690.43 nm (f = 0.0023). [d] The calculated spectrum shows a transition of lower intensity at 696.39 nm (f = 0.0053). [e] The calculated spectrum shows three transitions of similar intensity at 711.43 nm (f = 0.0019), 595.44 nm (f = 0.0019) and 519.50 nm (f = 0.0016). [f] The calculated spectrum shows a transition of lower intensity at 902.15 nm (f = 0.0006). [g] The calculated spectrum shows a transition of higher intensity at 1089.0 nm (f = 0.0035).

In previous work on the Cu^{2+}–L1 system, a linear dependence between the maximum in the electronic spectrum (λ_{max}) of each structure and its corresponding τ parameter was found.[7] In this work, the whole set of data in Table 2 also led to a similar dependence between λ_{max} and τ [Figure 9, Equation (9)], although the r^2 value is smaller. Moreover, the numerical values in Equation (9) are very similar to those found for the Cu–L1 system,[7] which seems to indicate that the correlation is independent of the nature and dentate character of the ligand and supports the general idea that tbp structures show higher λ_{max} than sp structures.

$$\lambda_{max} = 577\tau + 311 \ (r^2 = 0.82) \quad (9)$$

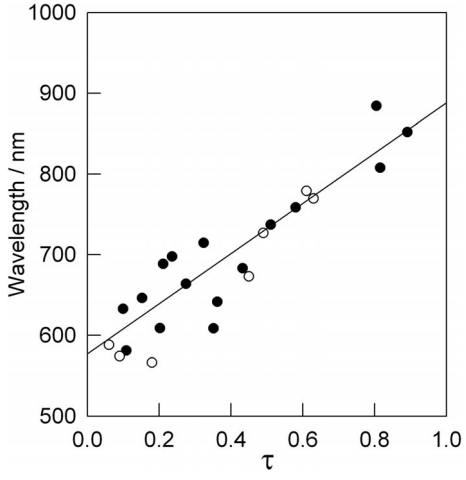

Figure 9. Plot showing the correlation between the λ_{max} [nm] and τ values for the different optimized geometries obtained for the Cu^{2+}–tren system (●). For comparison, the values for the related L1 complexes have been plotted (○), although they were not used to define the correlation in Equation (9).

Optimizations for the CuL^{2+} species with the ligand acting as tetradentate led to the CuL-*a* geometry as the most stable one and according to its τ value (0.43) it has a geometry intermediate between trigonal bipyramid and square pyramidal. However, the position of the absorption maximum for this geometry is far from the experimental observation and different optimizations starting from geometries with minor structural changes with respect to CuL-*a* led to structures with close energy but very different τ and λ_{max} values (see structures CuL-*b* and CuL-*c* in Table 2), which are in better agreement with the experimental spectrum and the reported crystal structures for Cu^{2+} complexes with tetradentate tren.[6] For this reason, the CuL^{2+}-*a* geometry was employed as a starting point for the modification of its τ value and to check the changes in the relative energies of the resulting structures. Calculations were carried out by fixing one of the Cu–N–N–N dihedral angles that has a direct effect on the τ value and optimizing the rest of the

molecule in solution. The results are summarized in Figure 10, which shows that there is a wide range of τ values (ca. 0.30–0.85) in which the optimized structures have very close relative energies. Therefore, this flat potential energy surface prevents the precise determination of the solution geometry of the CuL^{2+} species. Flat potential energy surfaces are not very surprising as they have already been obtained theoretically for several Cu^{II}–triamine complexes.[39] Interestingly, although Figure 10 corresponds to data for $CuL(H_2O)^{2+}$, the range of τ values with energies close to the minimum is very similar to the range found for crystal structures of $CuLX^{z+}$ complexes, where X is a monodentate ligand (τ = 0.46–1.00).[6] Combination of Figures 9 and 10 indicates that formation of different species with a wide range of λ_{max} can occur in solution due to the small energy difference between structures with very different τ values, the actual structure is determined by additional factors, such as specific interactions with the solvent, which were not included in the calculations.

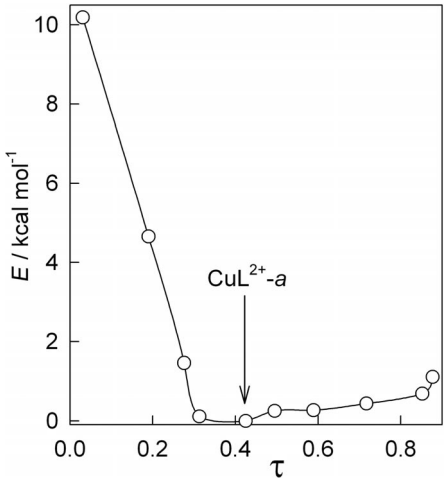

Figure 10. The relative energy of the geometries obtained from the CuL^{2+}-*a* species after modifying its τ parameter by changing one of the Cu–N–N–N dihedral angles.

Additional calculations were carried out for the CuL^{2+} species with tren acting as tridentate and the geometries named as CuL^{2+}-*d*, CuL^{2+}-*e*, CuL^{2+}-*f* and CuL^{2+}-*g* in Table 2 were obtained. These structures have essentially a square pyramidal character and are very similar to each other, the major difference lies in the position of the uncoordinated ligand arm. It is important to note that there is a difference of only 5.5 kcal mol^{-1} between the two most stable structures with tetra- and tridentate tren, namely the CuL^{2+}-*a* and CuL^{2+}-*d* species, which indicates that the energetic cost of the hydrolysis of one of the Cu–N bonds is small in aqueous solution and that formation of a mixture of both species is possible. Nevertheless, in contrast to the related Cu^{2+}–L1 system, where coexistence of two species in equilibrium was revealed in the kinetic studies, in the case of tren there is no experimental evidence for the formation of such a mixture. However, the calculated energy change associated with hydrolysis in the L1 system is smaller (3.2 kcal mol^{-1}), which makes the hydrolysis equilibrium more displaced towards the formation of the species with the tridentate ligand.[7]

The DFT study of $CuLOH^+$ species shows the existence of three structures with very close energies. According to the calculations, $CuLOH^+$-*a* is the most stable structure and shows a geometry that is intermediate between trigonal bipyramid and square pyramidal (τ = 0.35), while $CuLOH^+$-*b* is trigonal bipyramidal (τ = 0.82) and is only 1.0 kcal mol^{-1} higher in energy. Above them, at 3.6 kcal mol^{-1}, there is another square pyramidal structure ($CuLOH^+$-*c*, τ = 0.21) that is quite similar to $CuLOH^+$-*a*. Structures that contain tridentate tren were also optimized, but they are not included because of their higher relative energy (more than ca. 12 kcal mol^{-1}). The electronic spectra calculated for these geometries are compared with the experimental spectrum in Figure 11. Figure 11 and the EPR spectrum for this species, which is typical of tbp complexes without any evidence of mixture with sp species, suggest that the CuLOH-*b* geometry is the one favoured in solution.

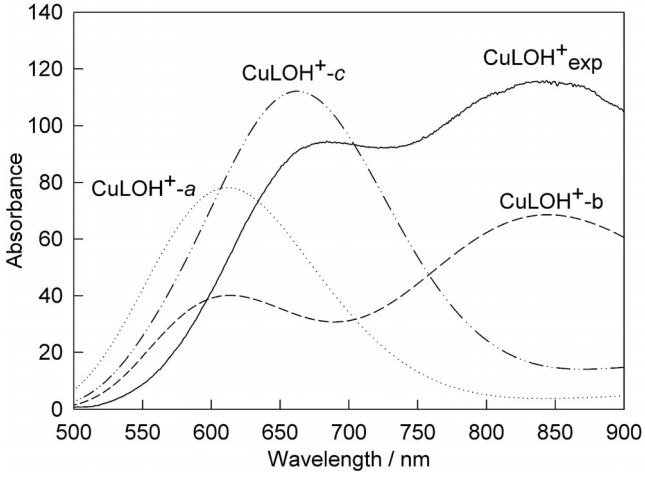

Figure 11. Experimental absorption spectrum of $CuLOH^+$ complexes obtained from analysis of spectophotometric titration and TD-DFT calculated absorption spectra of CuLOH-*a*, CuLOH-*b* and CuLOH-*c* at a full width at half maximum of 3000 cm^{-1}.

For the $HCuL(H_2O)_2^{3+}$ species, five geometries that are close in energy were obtained (Table 2). All of them had τ values that are typical of sp complexes or are intermediate between tbp and sp and four of them ($HCuL^{3+}$-*a*, $HCuL^{3+}$-*c*, $HCuL^{3+}$-*d* and $HCuL^{3+}$-*e*) had calculated spectra that showed a single transition in the 550 to 750 nm range, which could explain the band at 660 nm in the experimental spectrum (Figure 1). Interestingly, the reported[16a] crystal structure of $[Cu(HLCl_2)](ClO_4)\cdot H_2O$ indicates a τ value of 0.08, which is very close to the values in Table 2 for the two most stable geometries found for this species. The remaining isomer, $HCuL^{3+}$-*b*, which is only 3.0 kcal mol^{-1} less stable than $HCuL^{3+}$-*a*, shows three different absorption transitions of similar intensity that could be responsible for the flat part of the absorption spectrum of $HCuL^{3+}$. However, it must be remembered that the calculation errors for the experimental spectrum are large in this case because it is only a minor species in solution and so the flat part of

that spectrum could also result from the accumulation of experimental and calculation errors. With regards to the intermediate I formed during the acid-promoted decomposition of all of the Cu^{2+}–tren complexes, the experimental spectrum with a maximum at 630 nm is compatible with a $HCuL^{3+}$ species, such as those included in Table 2. However, as there is the possibility that this intermediate correspond to a species with a higher degree of protonation, optimizations were also carried out for $H_2CuL(H_2O)_3^{4+}$ and $H_3CuL(H_2O)_4^{5+}$. The results are included in Table 2 and the most stable geometry found for each species is shown in Figure 8. Although a transition within the 600 to 700 nm range was calculated for most of the optimized geometries for these species, it is usually accompanied of another transition at higher wavelengths (900–1100 nm), which was not observed experimentally (Figure 3). Moreover, the calculated spectra in the Supporting Information show a gradual decrease in the intensity of the absorption band as the protonation state increases, thus the experimental spectrum of I in Figure 3 fits better with the spectra calculated for the different $HCuL^{3+}$ species. Nevertheless, the results of the DFT and TD-DFT calculations were not able to unequivocally determine if intermediate I is a $HCuL^{3+}$ species that is different from the one detected in the equilibrium studies or if it is a species with a higher protonation state for which the electronic transition that was calculated in the near infrared was absent or shifted out of the detector range.

Conclusions

The solution chemistry of Cu^{2+}–tren complexes was explored both from an experimental and theoretical point of view. Equilibrium studies indicate that aqueous solutions contain different amounts of the $HCuL^{3+}$, CuL^{2+} and $CuL(OH)^{+}$ species, which can be differentiated by their electronic and EPR spectra. According to its spectrum, CuL^{2+} has a tbp structure, which is in agreement with crystal diffraction data for Cu^{2+} complexes with tetradentate tren.[6] However, there are alternative structures that do not differ very much in energy, and it was previously found[7] that the related complex with the substituted L1 ligand exists as an equilibrium mixture of the $CuL1(H_2O)^{2+}$ and $CuL1(H_2O)_2^{2+}$ complexes in which L1 is tetra- and tridentate, respectively.

Although the structure of $CuL(H_2O)^{2+}$ is usually described as tbp, there are significant distortions, and crystal diffraction data indicate that Cu^{2+}–tren complexes show τ values between 1 and ca. 0.5, that is, from ideal tbp geometry to a structure that is intermediate between tbp and sp. The DFT calculations are in agreement with these crystal data, although there is a wide range of τ values with very small energy differences, which indicates that the actual structure in solid state can be determined by crystal-packing interactions and in solution by interactions with the solvent. The previously proposed correlation between the τ values and the TD-DFT estimation of the absorption maximum in the electronic spectrum[7] was confirmed and it can be used to estimate the degree of distortion for the solution structure. In the course of the acid-promoted decomposition of the $CuL(H_2O)^{2+}$ complex, an intermediate with a spectrum that is typical of sp structures is formed. Although the data did not allow for the determination of whether it is a $HCuL^{3+}$ species or a higher protonated complex, the shift in the absorption band clearly indicates that reducing the dentate character of tren leads to a structural change to sp, which is also supported by the EPR spectra and the theoretical calculations.

In basic solutions, $CuL(H_2O)^{2+}$ converts to $CuL(OH)^{+}$, which shows an electronic spectrum with two absorption bands in positions that are typical of tbp and sp structures. Although the DFT and TD-DFT calculations indicated that they can be the result of contributions of different geometries with close energy values, no evidence of differentiated behaviour for both of the bands was obtained. Moreover, the EPR spectrum is typical of tbp species without a significant contribution from sp complexes. Thus, it appears that both of the bands correspond to different transitions for a single tbp compound. On the other hand, $CuL(H_2O)^{2+}$ coexists in acidic aqueous solution with the protonated $HCuL(H_2O)_2^{3+}$ species, which also shows an electronic spectrum with unequivocal contribution from the sp geometry. The most stable of the optimized geometries for this species shows a τ value of 0.11 and a calculated λ_{max} of 581 nm, which are in reasonable agreement with the experimental observation.

The whole set of results in the present and previous works indicate that although the chemistry of tren and related ligands is dominated by the tbp geometry, sp species are formed under certain conditions. Square pyramidal geometry appears to be not only relevant for species where the ligand is hypodentate (such as protonated complex species) but also for ligands in which substituents are introduced in one of the terminal amino groups [for example, the $CuL1(H_2O)^{2+}$ species]. As the energy difference between both of the geometries and the energy changes associated to large structural distortions are not very large in general, subtle changes in the nature of the complex are expected to lead to geometry changes, so that the relevance of the sp geometry in the chemistry of these complexes can be larger than usually assumed from the tripodal character of the ligand.

Experimental Section

Equilibrium and Spectroscopic Studies

The KOH solutions used for the potentiometric titrations were obtained from Aldrich and titrated with potassium hydrogen phthalate. Solutions of Cu^{2+} were prepared from $Cu(NO_3)_2$ and were analyzed by ICP. The protonation constants of the ligand and the formation constants of ligand–Cu complexes were determined from several potentiometric titrations that were carried out at 25.0 ± 0.1 °C under N_2 with solutions that contained L and Cu^{2+} in a 1:1 molar ratio and the amount of $NaClO_4$ required to achieve a 0.15 M concentration of the supporting electrolyte. The pH read-

ings were obtained with a Crison GLP22+ instrument that was provided with a combined electrode. The system was calibrated to measure pH as $-\log[H^+]$ by titrating a concentrated $HClO_4$ solution with KOH and by using the Gran's plot to determine the standard potential and the ionic product of water (13.78).[40] The range of pH covered in the different titrations expanded from ca. 3 to 11, and the data were analyzed with the program HYPERQUAD.[41] The species distribution curves were obtained with the program HYSS. The spectrophotometric titration was performed by monitoring the pH with the Crison GLP22+ instrument and by recording the absorption spectra with a Cary 50-Bio spectrophotometer. The data were analyzed with SPECFIT.[42]

X-band electron paramagnetic resonance (EPR) measurements were performed at 100 K with a Bruker EMX spectrometer that was equipped with an ER-4192 ST Bruker cavity and an ER-4131 VT with the following parameters: microwave power 0.695 mW, modulation amplitude 3 G, modulation frequency 100 kHz. The EPR parameters were determined based on simulations that were performed with the EasySpin program.[43] The samples were prepared from an aqueous solution that contained $Cu(NO_3)_2$ and tren in a 1:1 molar ratio and the pH was then adjusted by addition of $NaOH/HClO_4$ to values selected from the species distribution curves that were derived from potentiometric data. Some pH values could be selected such that the solution contained a single species, but in other cases, especially for the $HCuL^{3+}$ species, it was only possible to prepare solutions that contained mixtures with other species. In this case some handling of the measured spectra was necessary in order to obtain the spectrum of the required species. Each solution was frozen at 77 K before the spectrum was measured. The spectra for the different species were estimated from the spectra recorded in strongly acidic (Cu_{aq}^{2+}) or basic [$CuL(OH)^+$] conditions, or by subtracting the contribution of these species to the mixtures that contained them with CuL^{2+} or $HCuL^{3+}$.

Kinetic Studies

The kinetic experiments were conducted at 25.0 ± 0.1 °C in the presence of 0.15 M supporting electrolyte with either a Cary 50-BIO spectrophotometer or an Applied Photophysics SX17MV stopped-flow instrument that was provided with a PDA-1 diode array detector. In both cases, the kinetic experiments provided spectral changes with time that were analyzed by using global analysis procedures with the SPECFIT software.[42] All of the solutions for the kinetic work on complex decomposition contained Cu^{2+} and the ligand in a 1:1 molar ratio ($[Cu]_0 = [L]_0 = 2 \times 10^{-3}$ M). The pH was adjusted with NaOH to values at which the species distribution curves indicated that the concentration of the $HCuL^{3+}$, $CuL^{2+}$and $CuLOH^+$ complexes achieved a maximum in solution. For kinetic studies on complex formation, a solution of the ligand ($[L]_0 = 4 \times 10^{-3}$ M), whose pH had been previously adjusted with $HClO_4$ or NaOH solutions, was mixed in the stopped-flow instrument with a solution that contained the same concentration of Cu^{II} with the pH adjusted to the same value. No buffers were added because it has been previously shown that buffering agents can interact with either the metal ion or the protonated forms of polyamine ligands.[27] Because of the absence of buffers, the complex formation reactions occurred with changes in the concentration of the protons, which were taken into account by introducing them in the kinetic model that was used to analyze the data. In order to analyze the effects associated with the interaction with nitrate, some experiments on complex formation and decomposition were carried out under conditions that are different from those described above, the precise details for each case are given in the corresponding sections.

Computational Details

All DFT calculations were carried out with the Gaussian 03 software package[44] by using the B3LYP hybrid functional.[45] The Stuttgart-Dresden SDD basis set[46] was used with a relativistic effective core potential for Cu, and all of the ligand atoms (C, N, O, H) were described by the Pople-style basis set 6-31+G(d,p).[47] Test calculations with the nonhybrid BP86 functional gave very similar results and so the hybrid B3LYP functional was used to enable comparison with previous work.[7] All of the geometry optimizations were performed without any symmetry constraints and efforts were made to find the lowest energy conformations by comparing the structures optimized from different starting geometries. Optimizations were performed in aqueous phase (ε = 78.39) through the conductor-like polarizable continuum model (CPCM)[38] as implemented in Gaussian 03.[44]

The electronic absorption spectra of the previously optimized species were calculated at the same theory level with the time-dependent DFT (TD-DFT) formalism[48] and 30 singlet-excited-state energies were calculated for each complex. The nonspecific solvent effect was also considered in the TD-DFT calculations by means of the nonequilibrium version of the CPCM algorithm.[38] No attempts were made to improve the quality of the computational results by using semiempirical methods (DFT with tuned hybrid functionals or a variation of the nuclear charge of the metal centre) because those methodologies need to be optimized for each type of compound and molecular property,[49] which was beyond the scope of this work.

Supporting Information (see footnote on the first page of this article): Table and figures with additional experimental data, Cartesian Coordinates, absolute energy and TD-DFT calculated electronic spectra for all of the species discussed in the text.

Acknowledgments

Financial support by the Spanish Ministerio de Ciencia e Innovación (MICINN) (project number CTQ2009-14443-C02-01) and Junta de Andalucía (FQM-137), and computing facilities provided by Centro de Supercomputación de la Universidad de Cádiz are gratefully acknowledged. A. G. A. also acknowledges a postdoctoral grant from the MICINN.

[1] a) P. Comba, T. W. Hambley, M. A. Hitchman, H. Stratemeier, *Inorg. Chem.* **1995**, *34*, 3903–3911; b) B. J. Hathaway, *J. Chem. Soc., Dalton Trans.* **1972**, 1196–1199; c) B. J. Hathaway, D. E. Billing, *Coord. Chem. Rev.* **1970**, *5*, 143–207.

[2] a) P. Comba, A. M. Sargeson, L. M. Engelhardt, J. M. Harrowfield, A. H. White, E. Horn, M. R. Snow, *Inorg. Chem.* **1985**, *24*, 2325–2327; b) P. V. Bernhardt, R. Bramley, L. M. Engelhardt, J. M. Harrowfield, D. C. R. Hockless, B. R. Korybut-Daszkiewicz, E. R. Krausz, T. Morgan, A. M. Sargeson, *Inorg. Chem.* **1995**, *34*, 3589–3599; c) P. Comba, C. Haaf, H. Wadepohl, *Inorg. Chem.* **2009**, *48*, 6604–6614.

[3] a) E. V. Rybak-Akimova, A. Y. Nazarenko, L. Chen, P. W. Krieger, A. M. Herrera, V. V. Tarasov, P. D. Robinson, *Inorg. Chim. Acta* **2001**, *324*, 1–15; b) J. P. Schneider, J. W. Kelly, *J. Am. Chem. Soc.* **1995**, *117*, 2533–2546; c) R. Kannappan, S. Tanase, I. Mutikainen, U. Turpeinen, J. Reedijk, *Inorg. Chim. Acta* **2005**, *358*, 383–388.

[4] a) N. Kitajima, K. Fujisawa, Y. Morooka, *J. Am. Chem. Soc.* **1990**, *112*, 3210–3212; b) R. C. Elder, M. C. Hill, *Inorg. Chem.* **1979**, *18*, 729–732.

[5] a) S. R. Batten, B. F. Hoskins, B. Moubaraki, K. S. Murray, R. Robson, *Chem. Commun.* **2000**, *13*, 1095–1096; b) T. Osako,

K. D. Karlin, S. Itoh, *Inorg. Chem.* **2005**, *44*, 410–415; c) M. Meyer, L. Fremond, E. Espinosa, R. Guilard, Z. P. Ou, K. M. Kadish, *Inorg. Chem.* **2004**, *43*, 5572–5587; d) K. Miyoshi, H. Tanaka, E. Kimura, S. Tsuboyama, S. Murata, H. Shimizu, K. Ishizu, *Inorg. Chim. Acta* **1983**, *78*, 23–30; e) R. M. Nunes, R. Delgado, M. F. Cabral, J. Costa, P. Brandao, V. Felix, B. J. Goodfellow, *Dalton Trans.* **2007**, 4536–4545; f) H. Nagao, N. Komeda, M. Mukaida, M. Suzuki, K. Tanaka, *Inorg. Chem.* **1996**, *35*, 6809–6815; g) E. J. Laskowski, D. M. Duggan, D. N. Hendrickson, *Inorg. Chem.* **1975**, *14*, 2449–2459.

[6] A. G. Blackman, *Polyhedron* **2005**, *24*, 1–39.

[7] A. G. Algarra, M. G. Basallote, C. E. Castillo, M. P. Clares, A. Ferrer, E. García-España, J. M. Llinares, M. A. Mañez, C. Soriano, *Inorg. Chem.* **2009**, *48*, 902–914.

[8] A. Pasquarello, I. Petri, P. S. Salmon, O. Parisel, R. Car, E. Toth, D. H. Powell, H. E. Fischer, L. Helm, A. E. Merbach, *Science* **2001**, *291*, 856–859.

[9] S. Alvarez, M. Llunell, *J. Chem. Soc., Dalton Trans.* **2000**, 3288–3303.

[10] a) Z. D. Wang, W. Han, F. Bian, Z. Q. Liu, S. P. Yan, D. Z. Liao, Z. H. Jiang, P. Cheng, *J. Mol. Struct.* **2005**, *733*, 125–131; b) M. J. Rosales, R. A. Toscano, M. A. Luna-Canut, M. E. Sosa-Torres, *Polyhedron* **1989**, *8*, 909–915; c) F. A. Mautner, R. Vicente, S. S. Massoud, *Polyhedron* **2006**, *25*, 1673–1680; d) C. Gerard, A. Mohamadou, J. Marrot, S. Brandes, A. Tabard, *Helv. Chim. Acta* **2005**, *88*, 2397–2412; e) Z. D. Georgousis, P. C. Christidis, D. Hadjipavlou-Litina, C. A. Bolos, *J. Mol. Struct.* **2007**, *837*, 30–37.

[11] a) S. Tyagi, B. J. Hathaway, *J. Chem. Soc., Dalton Trans.* **1983**, 199–203; b) F. Thaler, C. D. Hubbard, F. W. Heinemann, R. van Eldik, S. Schindler, I. Fabian, A. M. Dittler-Klingemann, F. E. Hahn, C. Orvig, *Inorg. Chem.* **1998**, *37*, 4022–4029; c) R. C. Slade, A. A. G. Tomlinson, B. J. Hathaway, D. E. Billing, *J. Chem. Soc. A* **1968**, 61; d) R. Kuroda, S. F. Mason, T. Prosperi, S. Savage, G. E. Tranter, *J. Chem. Soc., Dalton Trans.* **1981**, 2565–2572.

[12] a) M. Duggan, N. Ray, B. Hathaway, G. Tomlinson, P. Brint, K. Pelin, *J. Chem. Soc., Dalton Trans.* **1980**, 1342–1348; b) A. Marzotto, A. Ciccarese, D. A. Clemente, G. Valle, *J. Chem. Soc., Dalton Trans.* **1995**, 1461–1468.

[13] a) C. C. Su, W. S. Lu, T. Y. Hui, T. Y. Chang, S. L. Wang, F. L. Liao, *Polyhedron* **1993**, *12*, 2249–2259; b) S. S. Massoud, F. A. Mautner, M. A. M. Abu-Youssef, N. M. Shuaib, *Polyhedron* **1999**, *18*, 2061–2067.

[14] a) T. S. Roche, R. G. Wilkins, *J. Am. Chem. Soc.* **1974**, *96*, 5082–5086; b) H. Stunzi, D. Perrin, T. Teitei, R. Harris, *Aust. J. Chem.* **1979**, *32*, 21–30; c) G. Anderegg, V. Gramlich, *Helv. Chim. Acta* **1994**, *77*, 685–690; d) R. J. Motekaitis, A. E. Martell, D. A. Nelson, *Inorg. Chem.* **1984**, *23*, 275–283; e) G. Anderegg, *Inorg. Chim. Acta* **1986**, *25*, 111; f) C. R. Bertsch, W. C. Fernelius, B. P. Block, *J. Phys. Chem.* **1958**, *62*, 444–450; g) R. J. Motekaitis, A. E. Martell, J. M. Lehn, E. I. Watanabe, *Inorg. Chem.* **1982**, *21*, 4253–4257.

[15] a) A. D. P. Paoletti, A. Vacca, *Inorg. Chem.* **1968**, *7*, 865–870; b) G. Golub, A. Lashaz, H. Cohen, P. Paoletti, B. Andrea, B. Valtancoli, D. Meyerstein, *Inorg. Chim. Acta* **1997**, *255*, 111–115; c) H. Keypour, M. Dehdari, S. Salehzadeh, K. P. Wainwright, *Trans. Met. Chem.* **2003**, *28*, 425–429.

[16] a) D.-Z. Niu, H.-J. Ma, F. Gao, Z.-S. Lu, J.-T. Chen, *Chin. J. Struct. Chem.* **2006**, *25*, 1457–1460; b) C.-H. Chen, J.-W. Cai, X.-M. Chen, *Acta Crystallogr., Sect. C* **2002**, *58*, m59–m60.

[17] Z. W. Mao, G. Liehr, R. van Eldik, *J. Chem. Soc., Dalton Trans.* **2001**, 1593–1600.

[18] a) A. W. Addison, H. M. J. Hendriks, J. Reedijk, L. K. Thompson, *Inorg. Chem.* **1981**, *20*, 103–110; b) M. Duggan, N. Ray, B. Hathaway, G. Tomlinson, P. Brint, K. Pelin, *J. Chem. Soc., Dalton Trans.* **1980**, 1342–1348; c) K. Takahashi, E. Ogawa, N. Oishi, Y. Nishida, S. Kida, *Inorg. Chim. Acta* **1982**, *66*, 97–103; d) L. Morpurgo, R. Falcioni, G. Rotilio, A. Desideri, B. Mondovi, *Inorg. Chim. Acta* **1978**, *28*, L141–L143.

[19] a) A. Mendoza, J. Aguilar, M. G. Basallote, L. Gil, J. C. Hernandez, M. A. Máñez, E. García-España, L. Ruiz-Ramirez, C. Soriano, B. Verdejo, *Chem. Commun.* **2003**, 3032–3033; b) J. Aguilar, M. G. Basallote, L. Gil, J. C. Hernandez, M. A. Máñez, E. García-España, C. Soriano, B. Verdejo, *Dalton Trans.* **2004**, 94–103.

[20] a) L. Raehm, J. P. Sauvage, *Molecular Machines And Motors, Vol. 99*, Springer-Verlag, New York, **2001**, pp. 55–78; b) M. G. Basallote, J. Duran, M. J. Fernández-Trujillo, M. A. Máñez, *J. Chem. Soc., Dalton Trans.* **1999**, 3817–3823; c) W. J. Lan, C. S. Chung, *J. Chem. Soc., Dalton Trans.* **1994**, 191–194; d) R. W. Hay, M. T. H. Tarafder, M. M. Hassan, *Polyhedron* **1996**, *15*, 725–732; e) R. W. Hay, M. P. Pujari, F. McLaren, *Inorg. Chem.* **1984**, *23*, 3033–3035; f) R. W. Hay, R. Bembi, W. T. Moodie, P. R. Norman, *J. Chem. Soc., Dalton Trans.* **1982**, 2131–2136; g) G. DeSantis, L. Fabbrizzi, A. Perotti, N. Sardone, A. Taglietti, *Inorg. Chem.* **1997**, *36*, 1998–2003; h) N. F. Curtis, S. R. Osvath, *Inorg. Chem.* **1988**, *27*, 305–310; i) M. G. Basallote, J. Duran, M. J. Fernández-Trujillo, M. A. Máñez, *J. Chem. Soc., Dalton Trans.* **2002**, 2074–2079; j) A. R. Pease, J. O. Jeppesen, J. F. Stoddart, Y. Luo, C. P. Collier, J. R. Heath, *Acc. Chem. Res.* **2001**, *34*, 433–444; k) K. Kinbara, T. Aida, *Chem. Rev.* **2005**, *105*, 1377–1400; l) M. G. Rossmann, V. V. Mesyanzhinov, F. Arisaka, P. G. Leiman, *Curr. Opin. Struct. Biol.* **2004**, *14*, 171–180.

[21] C. Bazzicalupi, A. Bencini, A. Bianchi, A. Danesi, C. Giorgi, B. Valtancoli, *Inorg. Chem.* **2009**, *48*, 2391–2398.

[22] a) R. A. Read, D. W. Margerum, *Inorg. Chem.* **1981**, *20*, 3143–3149; b) D. W. Margerum, G. R. Cayley, D. C. Weatherburn, G. K. Pagenkopf, *ACS Monograph* **1978**, *174*, 1; c) J. H. Espenson, *Chemical Kinetics and Reaction Mechanism*, 2nd ed., McGraw-Hill, New York, **1995**, pp. 102–103.

[23] S. Siddiqui, R. E. Shepherd, *Inorg. Chem.* **1983**, *22*, 3726–3733.

[24] J. K. Walker, R. Nakon, *Inorg. Chim. Acta* **1981**, *55*, 135–140.

[25] a) H. B. Jonassen, T. H. Dexter, *J. Am. Chem. Soc.* **1949**, *71*, 1553–1556; b) R. G. Wilkins, *J. Chem. Soc.* **1962**, 4475–4478.

[26] N. McCann, G. A. Lawrance, Y. M. Neuhold, M. Maeder, *Inorg. Chem.* **2007**, *46*, 4002–4009.

[27] M. G. Basallote, J. Duran, M. J. Fernández-Trujillo, M. A. Máñez, B. Szpoganicz, *J. Chem. Soc., Dalton Trans.* **1999**, 1093–1100.

[28] The possibility that the observed rate constant would not correspond to slow complex formation between Cu^{2+} and H_3L^{3+} but to a faster reaction of the metal with a ligand species in a lower protonation state, such as H_2L^{2+}, can be reasonably ruled out because the concentration of H_2L^{2+}, as well as of HL^+ or L, change significantly with pH, so that some change in k_{obs} with pH should be observed.

[29] M. Soibinet, D. Gusmeroli, L. Siegfried, T. A. Kaden, C. Palivan, A. Schweiger, *Dalton Trans.* **2005**, 2138–2146.

[30] a) D. B. Moss, C.-T. Lin, D. B. Rorabacher, *J. Am. Chem. Soc.* **1973**, *95*, 5179–5185; b) T. Biver, F. Secco, M. R. Tinè, M. Venturini, *J. Inorg. Biochem.* **2004**, *98*, 33–40.

[31] a) A. De Robertis, C. De Stefano, C. Foti, G. Signorino, *Talanta* **1997**, *44*, 1839–1846; b) A. Odani, H. Masuda, K. Inukai, O. Yamauchi, *J. Am. Chem. Soc.* **1992**, *114*, 6294–6300; c) J. Gulens, P. K. Leeson, L. Séguin, *Anal. Chim. Acta* **1984**, *156*, 19–31; d) R. N. Sylva, M. R. Davidson, *J. Chem. Soc., Dalton Trans.* **1979**, 232–235.

[32] L. A. McDowell, H. L. Johnston, *J. Am. Chem. Soc.* **1936**, *58*, 2009–2014.

[33] a) M. J. Fernández-Trujillo, B. Szpoganicz, M. A. Mañéz, L. T. Kist, M. G. Basallote, *Polyhedron* **1996**, *15*, 3511–3517; b) C.-T. Lin, D. B. Rorabacher, G. R. Cayley, D. W. Margerum, *Inorg. Chem.* **1975**, *14*, 919–925.

[34] J. A. Drumhiller, F. Montavon, J. M. Lehn, R. W. Taylor, *Inorg. Chem.* **1986**, *25*, 3751–3757.

[35] R. G. Wilkins, *Kinetics and Mechanism of Reactions of Transition Metal Complexes*, 2nd ed., VCH Verlagsgesellschaft, Weinheim, Germany, **1991**.

[36] A preliminary study of the CuL^{2+} species has been reported previously in ref. [7].
[37] S. Salehzadeh, M. Bayat, *J. Comput. Chem.* **2010**, *31*, 2371–2380.
[38] M. Cossi, N. Rega, G. Scalmani, V. Barone, *J. Comput. Chem.* **2003**, *24*, 669–681.
[39] A. Bentz, P. Comba, R. J. Deeth, M. Kerscher, B. Seibold, H. Wadepohl, *Inorg. Chem.* **2008**, *47*, 9518–9527.
[40] G. Gran, *Analyst* **1952**, *77*, 661–671.
[41] P. Gans, A. Sabatini, A. Vacca, *Talanta* **1996**, *43*, 1739–1753.
[42] R. A. Binstead, B. Jung, A. D. Zuberbühler, *Spectrum Software Associates*, Chapel Hill, **2000**.
[43] S. Stoll, A. Schweiger, *J. Magn. Reson.* **2006**, *178*, 42–55.
[44] M. J. Frisch, G. W. Trucks, H. B. Schlegel, G. E. Scuseria, M. A. Robb, J. R. Cheeseman, J. A. J. Montgomery, T. Vreven, K. N. Kudin, J. C. Burant, J. M. Millam, S. S. Iyengar, J. Tomasi, V. Barone, B. Mennucci, M. Cossi, G. Scalmani, N. Rega, G. A. Petersson, H. Nakatsuji, M. Hada, M. Ehara, K. Toyota, R. Fukuda, J. Hasegawa, M. Ishida, T. Nakajima, Y. Honda, O. Kitao, H. Nakai, M. Klene, X. Li, J. E. Knox, H. P. Hratchian, J. B. Cross, C. Adamo, J. Jaramillo, R. Gomperts, R. E. Stratmann, O. Yazyev, A. J. Austin, R. Cammi, C. Pomelli, J. W. Ochterski, P. Y. Ayala, K. Morokuma, G. A. Voth, P. Salvador, J. J. Dannenberg, V. G. Zakrzewski, S. Dapprich, A. D. Daniels, M. C. Strain, O. Farkas, D. K. Malick, A. D. Rabuck, K. Raghavachari, J. B. Foresman, J. V. Ortiz, Q. Cui, A. G. Baboul, S. Clifford, J. Cioslowski, B. B. Stefanov, G. Liu, A. Liashenko, P. Piskorz, I. Komaromi, R. L. Martin, D. J. Fox, T. Keith, M. A. Al-Laham, C. Y. Peng, A. Nanayakkara, M. Challacombe, P. M. W. Gill, B. Johnson, W. Chen, M. W. Wong, C. Gonzalez, J. A. Pople, *Gaussian 03*, Revision E.01, Gaussian, Inc., Wallingford, CT, **2004**.
[45] a) A. D. Becke, *J. Chem. Phys.* **1993**, *98*, 5648–5652; b) C. T. Lee, W. T. Yang, R. G. Parr, *Phys. Rev. B* **1988**, *37*, 785–789.
[46] D. Andrae, U. Haussermann, M. Dolg, H. Stoll, H. Preuss, *Theor. Chim. Acta* **1990**, *77*, 123–141.
[47] A. Schaefer, H. Horn, R. Ahlrichs, *J. Chem. Phys.* **1992**, *97*, 2571–2577.
[48] M. E. Casida, C. Jamorski, K. C. Casida, D. R. Salahub, *J. Chem. Phys.* **1998**, *108*, 4439–4449.
[49] M. Atanasov, P. Comba, B. Martin, V. Müller, G. Rajaraman, H. Rohwer, S. Wunderlich, *J. Comput. Chem.* **2006**, *27*, 1263–1277, and references cited therein.

Received: January 24, 2012
Published Online: April 4, 2012

